EPR evidence for As interstitial-related defects in semi-insulating GaAs

E. Christoffel, T. Benchiguer, A. Goltzené, and C. Schwab
Groupe de Recherches Physiques et Matériaux, Centre de Recherches Nucléaires, Institut National de Physique Nucléaire et de Physique des Particules du Centre National de la Recherche Scientifique (IN2P3-CNRS), Université Louis Pasteur, 23 rue du Loess, 67037 Strasbourg CEDEX, France

Wang Guangyu and Wu Ju
Shanghai Institute of Metallurgy, Chinese Academy of Sciences, 865 Chang Ning Road, Shanghai 200050, China
(Received 28 June 1989; revised manuscript received 18 September 1989)

We report the analysis of the residual paramagnetic structure appearing in semi-insulating GaAs after microwave saturation of the As_{Ga}-related spectrum and most intense after preliminary plastic deformation of the material. It is separable into two similar and correlated central hyperfine partially resolved spectra of trigonal symmetry, both attributed to As interstitial-related defects. Some possibilities of suitable complexes, especially in the recent context of the EL2 identification with an As_{Ga}^{+}-As_i pair, are discussed.

INTRODUCTION

Besides the peculiar properties of the paramagnetic defects constrainable to the model of a singly ionized anion antisite As_{Ga}^{4+}, i.e., As_{Ga}^{+} in electrical notation, microwave-saturation experiments during regular electron-paramagnetic-resonance (EPR) investigations of semi-insulating GaAs also reveal some new features, such as the structure labeled ST,[1] which progressively emerges from under the third component of the As_{Ga}^{+} quadruplet at X-band frequencies. Though first suspected in electron-irradiated samples,[2] the ST spectrum seems strongest and best resolved in plastically deformed materials.

In fact for both particle irradiation[2,3] and plastic deformation,[4] the quantitative analysis of the As_{Ga}^{+} spectra already indicates the presence of correlated singlet lines at lower microwave-power levels; however, only association of deformation and high power level systematically revealed well-defined ST spectra, encouraging us to proceed to the determination of the electron and nuclear spins—the first step of an EPR identification of the corresponding defect.

This latter point is directly related to the nature of the acceptors which compensate the As_{Ga} donors. Indeed, as the fraction of paramagnetic As_{Ga}^{+} augments with deformation, the questions may be raised whether it is caused by an increase of antisites or by an increase of acceptors during this deliberate perturbation of the crystal. Also, the new acceptors are not necessarily the same as those present prior to deformation.

This paper reports the detailed EPR analysis of the ST structure in plastically deformed semi-insulating GaAs; it is separable into two spectra of trigonal symmetry, whose intensities remain correlated during both generation under increasing strain and thermal decay.

EXPERIMENTAL DETAILS AND DATA ANALYSIS

The materials used in this study have been prepared at the Shanghai Institute for Metallurgy. Further details on growth method and plastic deformation are given in Ref. 5.

Although the so-called ST structure may look similar in deformed and in electron-irradiated samples, the easier saturation of the As_{Ga}^{+} quadruplet facilitates its recognition in the former materials; therefore this work was restricted to strained materials.

The occurrence of ST is independent of the initial growth method (i.e., liquid-encapsulated Czochralski or horizontal Bridgman techniques) and of doping (Cr, In). As an illustration, Fig. 1 compared the EPR spectra of an undoped and an In-doped semi-insulting GaAs sample, both deformed to similar strain degrees and recorded with a microwave power $P=100$ mW at 4.2 K in the X band.

The ST structure is slightly anisotropic as shown on the rotation pattern of Fig. 2, taken around a $[1\bar{1}0]$ axis; for the sake of legibility, the As_{Ga}^{+} and cavity baseline contributions have been subtracted in the plotted spectra. The most significant change occurs at the high-field side of the fourth component. At first sight, for $\mathbf{H}_0 \| [001]$, it consists of an overlap of four identical lines.

Based on the latter observation, we have tried to describe the ST structure by an unpaired electron with electronic spin $S=\frac{1}{2}$ subjected to a central hyperfine interaction resulting from a nuclear spin $I=\frac{3}{2}$ nucleus, which effectively yields four identical components for one center. Neglecting the much weaker quadrupolar and nuclear Zeeman terms, the corresponding spin Hamiltonian is given by

$$\mathcal{H}=\beta \mathbf{H}_0 \cdot \underline{\mathbf{g}} \cdot \mathbf{S} + h \mathbf{S} \cdot \underline{\mathbf{A}} \cdot \mathbf{I} , \quad (1)$$

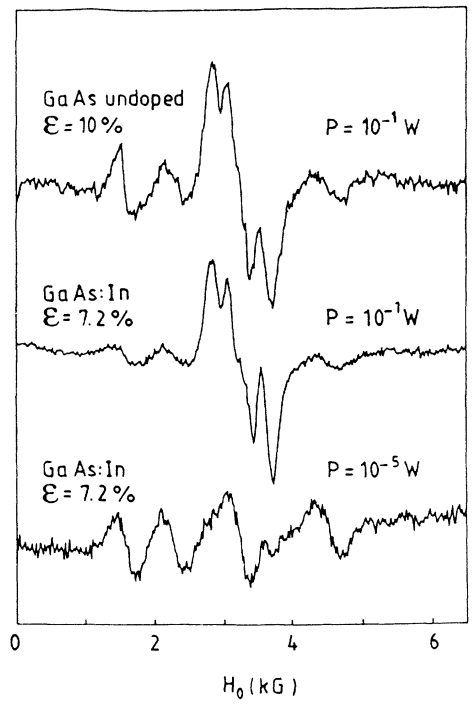

FIG. 1. High-microwave-power-level EPR recordings of plastically semi-insulating GaAs, revealing the same ST structure in undoped and In-doped materials, in comparison with a low-power recording mainly showing the As_{Ga}^{+} quadruplet (9 GHz, 4.2 K).

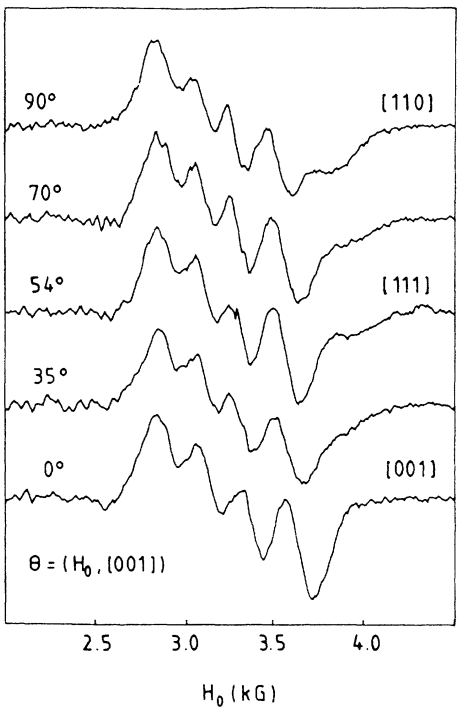

FIG. 2. Angular variation of the ST structure for a rotation around a binary axis of the crystal ($\mathbf{H}_0 \perp [\bar{1}10]$).

where $\underline{\mathbf{g}}$ and $\underline{\mathbf{A}}$ are, respectively, the g factor and hyperfine-coupling second-rank tensors. When analyzing the experimental spectra, we have, of course, to take into account the different equivalent orientations of the centers with respect to the host lattice.

According to relation (1), we have analyzed the simplest experimental spectrum, i.e., that for $\mathbf{H}_0 \| [001]$, in terms of a superposition of four independent Gaussian lines using the same multiparameter fitting method as developed in Ref. 3. Although their positions were set free, the fit did not result in four identical lines as predicted by relation (1). Instead, we obtained four dissimilar broad and overlapping lines, where the positive lobe of one was nearly superimposed with the negative one of the following line. The experimental structure merely results from this partial cancellation between positive and negative derivatives of the constrained Gaussians.

Irrespective of any further inclusion of a quadrupole effect, this result seems in contradiction with our initial hypothesis of an $(S=\frac{1}{2}; I=\frac{3}{2})$ hyperfine spectrum, which calls for four identical lines. However, the fit suggests that the two outer lines could possibly be related as their amplitude and width are closest. Associating them in the simplest way as an $(S=\frac{1}{2}; I=\frac{1}{2})$ doublet requires us to continue to deal with two dissimilar lines for describing the remaining two inner lines. Obviously, this approach involving a doublet and two independent singlets would then require ascription to three different defects in the most complicated case. It is discarded, as a simpler solution with only two defects is achievable.

Returning to our initial hypothesis of an $(S=\frac{1}{2}; I=\frac{3}{2})$ constraint, we try to link the outer lines in a different manner by assuming that the lowest- and highest-magnetic-field lines correspond to, respectively, the positive and negative lobes of the outer components of the expected quadruplet. This is achievable with a superposition of four equidistant and identical lines whose overlap then results in almost exact cancellation of the contributions in between the former lobes. A new fit under these conditions also unexpectedly returns a near equality for the two inner singlets. As will be shown later, the variation of the contour of these overlapping lines during rotation suggests that they too could result from an $(S=\frac{1}{2}; I=\frac{3}{2})$ hyperfine spectrum.

Having thus secured a starting point, we can analyze the angular variation of the spectra. Consider now axially symmetrical $\underline{\mathbf{g}}$ and $\underline{\mathbf{A}}$ tensors; for an arbitrary direction of the external magnetic field $\mathbf{H}_0$ with respect to crystal orientation, the possible degeneracies of the levels are lifted according to the different effective g_i and A_i values determined by the following set of equations:

$$\begin{aligned} g_i &= (g_{\|}^2 \cos^2\varphi_i + g_{\perp}^2 \sin^2\varphi_i)^{1/2} , \\ A_i &= (A_{\|}^2 \cos^2\varphi_i + A_{\perp}^2 \sin^2\varphi_i)^{1/2} , \end{aligned} \tag{2}$$

where φ_i is the angle between $\mathbf{H}_0$ and the axes i of the g and A ellipsoids defined by the constants $(g_{\|}, g_{\perp})$ and $(A_{\|}, A_{\perp})$.

In a cubic lattice a superposition of several quadruplets is then expected, weighted by the number of defects lying

along each direction i. The aforementioned simpler shape of the EPR spectrum for $\mathbf{H}_0 \| [001]$ suggests symmetry axes along trigonal crystal axes, as the transitions for these four equivalent axes then become degenerate. For any direction the experimental spectrum is a superposition of four spectra, where the φ_i $(i=1,2,3,4)$ designate the angles between $\mathbf{H}_0$ and each of the four ternary crystal axes.

The spectra for $\mathbf{H}_0 \| [111]$ and $\mathbf{H}_0 \| [110]$ are then analyzed correspondingly, constraining the different quadruplets defined by the parameters (g_i, A_i) of the set of Eqs. (2) and keeping the linewidth of each component as a common free parameter. Observation of a difference spectrum in close analogy with the initial one suggests the superimposition of two similar $(S=\frac{1}{2}; I=\frac{3}{2})$ spectra, which will be denoted ST1 and ST2. Figures 3–5 clearly indicate that each ST spectrum (solid circles) can be separated into two contributions of a similar contour; the second (ST2) is slightly shrunken with respect to the first one (ST1). The final error traces (lowest curves) show this approach to be at least consistent with the experimental data. In the same spirit, Fig. 6 shows the stability of the fitting parameters during analysis of the whole rotation pattern by the former simultaneous fit on both ST1 and ST2. Hence our choice of a solution involving only two centers seems justified. Table I lists the corresponding numerical values of the spin Hamiltonian parameters. As a result, this procedure was employed for analyzing the evolution of the ST structure during its generation and decay as follows.

GENERATION OF THE ST STRUCTURE

Concordant results have been reported for the generation of As_{Ga}^{+} centers during plastic deformation of undoped semi-insulating GaAs.[4,6] Indium doping induces only a more rapid increase easily explained in terms of a lattice hardening with the net consequence that more dislocations are created for the same strain value.[7] As already mentioned,[4] the As_{Ga}^{+} increase comes with an increase of a corresponding singlet for recordings at low microwave power. In fact, a similar behavior is observed for the generation of ST1 and ST2 recorded at a high power. Figure 7 shows the separate variations of the two

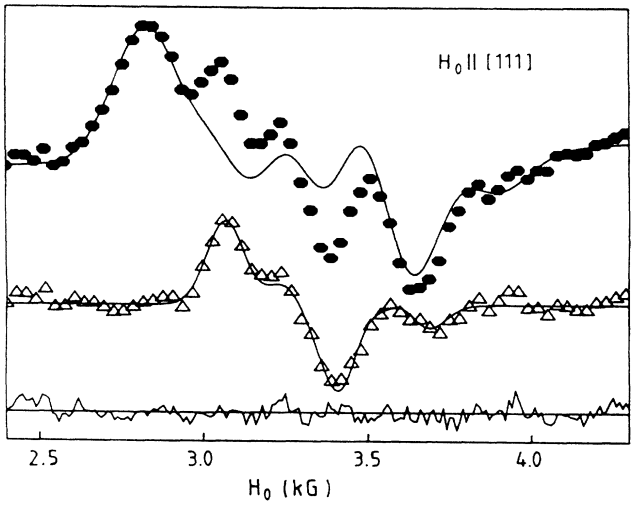

FIG. 4. Decomposition of the ST structure (circles) into a superposition of two trigonal spectra, ST1 and ST2 (solid lines), for the orientation $\mathbf{H}_0 \| [111]$. The difference spectra (triangles), obtained by subtraction of the fitted ST1 contribution from the original data, show the similarity between the ST1 and ST2 contours. The lower curves represent the final error traces.

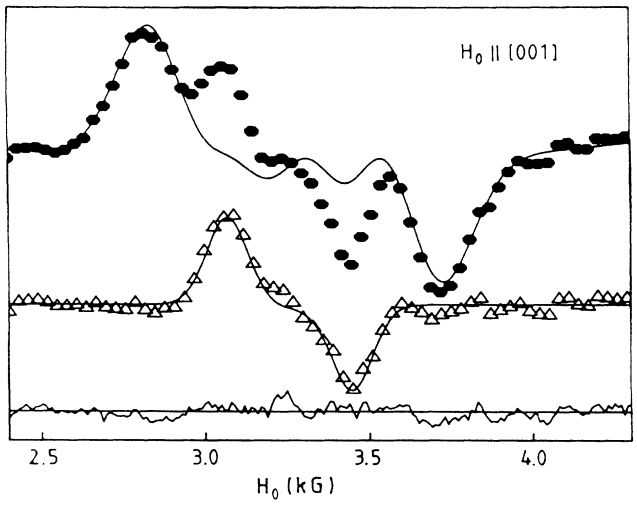

FIG. 3. Decomposition of the ST structure (circles) into a superposition of two trigonal spectra, ST1 and ST2 (solid lines), for the orientation $\mathbf{H}_0 \| [001]$. The difference spectra (triangles), obtained by subtraction of the fitted ST1 contribution from the original data, show the similarity between the ST1 and ST2 contours. The lower curves represent the final error traces.

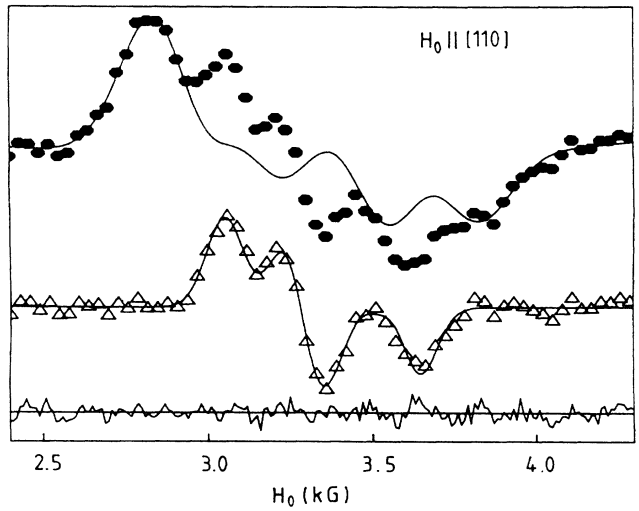

FIG. 5. Decomposition of the ST structure (circles) into a superposition of two trigonal spectra, ST1 and ST2 (solid lines), for the orientation $\mathbf{H}_0 \| [110]$. The difference spectra (triangles), obtained by subtraction of the fitted ST1 contribution from the original data, show the similarity between the ST1 and ST2 contours. The lower curves represent the final error traces.

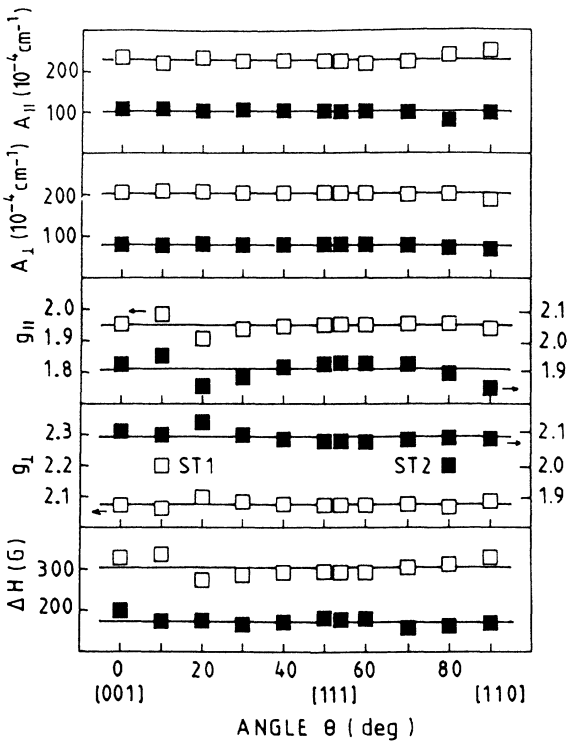

FIG. 6. Angular dependence of the spin Hamiltonian parameters for a decomposition of the ST structure into two trigonal specta, ST1 and ST2.

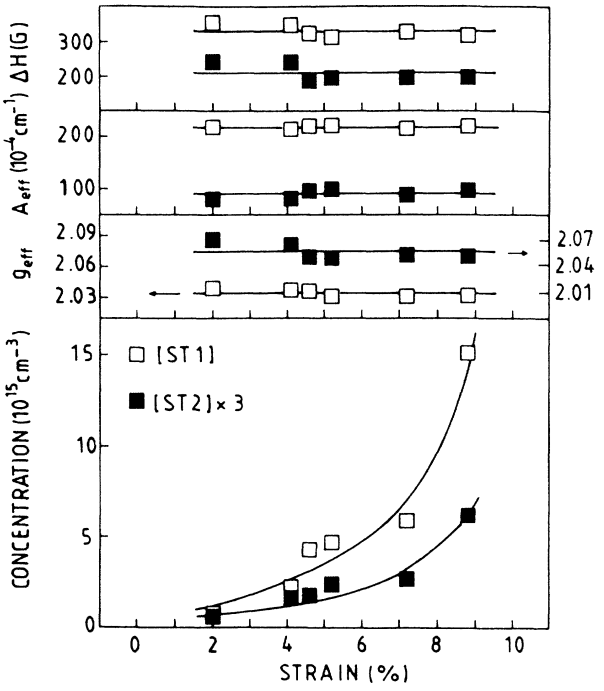

FIG. 7. Strain dependence of the ST1 and ST2 contents in plastically deformed GaAs:In and corresponding variations of the effective spin Hamiltonian parameters for $\mathbf{H}_0 \| [001]$.

as a function of strain for plastically deformed GaAs:In. They remain correlated over the whole strain range. The upper curves represent the corresponding variations of the effective spin Hamiltonian parameters as derived for a configuration $\mathbf{H}_0 \| [001]$. The scatter of the experimental data is compatible with the initial ST1 and ST2 decompositions.

THERMAL DECAY OF THE ST STRUCTURE

In an attempt to physically separate ST1 and ST2, we have analyzed their separate contributions during anneal of plastically deformed GaAs. A GaAs:In sample deformed to a strain degree of $\varepsilon = 8.8\%$ was successively annealed in 10-min isochronal steps under a purified Ar flow in a procedure similar to that used for neutron-irradiated material.[8] As plastic deformation is initially done at 400 °C,[5] the annealing steps start from this value. Figure 8 shows some physical temperature steps. The displayed spectra correspond to recordings where cavity baseline and residual As_{Ga}^{+} contributions have been subtracted. Besides the expected decrease of the ST structure, there is a dramatic increase of the X line,[8-10] which could not be removed even by a deep etch. Figure 9 shows the thermal decay of both ST1 and ST2 with the corresponding variations of the spin Hamiltonian parameters determined as before; again there is a remarkable stability over the whole range of investigation.

Contrary to our initial aim, ST1 and ST2 are not separable during thermal decay as are, for example, the As_{Ga}^{+} quadruplet and corresponding singlet in neutron-irradiated GaAs, nor do they behave differently under microwave saturation.[8] Instead, the ratio between the intensities is practically constant both during generation and thermal decay as shown by Fig. 10, where the ST1 intensity has been plotted versus that of ST2. A linear re-

TABLE I. Spin-Hamiltonian-parameter values of ST1 and ST2.

Defect	Hyperfine constant (10^{-4} cm^{-1}) $A_{\parallel}$	$A_{\perp}$	g factor $g_{\parallel}$	$g_{\perp}$	Linewidth (G) (FWHM)[a]
ST1	230±15	200±5	1.96±0.02	2.07±0.01	308±20
ST2	100±10	80±5	1.91±0.03	2.09±0.02	180±20

[a]Full width at half maximum.

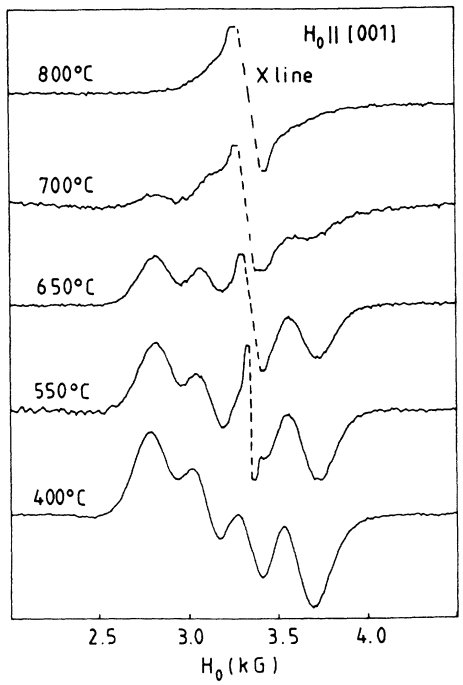

FIG. 8. Thermal decay of the ST structure induced in plastically deformed GaAs:In (9 GHz, 4.2 K).

gression yields a ratio $R \simeq 7.3$ within the assumption of $S=\frac{1}{2}$ states for both defects.

DISCUSSION

Our analysis of the ST structure rests on g and A ellipsoids aligned along the [111] directions. This leads to a degeneracy of all branches for $\mathbf{H}_0 \| [001]$, which is consistent with the observation of an apparent best-resolved spectrum with a minimum of components for this particular orientation. However, the mathematical fit does not allow us to relate all four components to a single defect with $I=\frac{3}{2}$. Instead, it shows that the ST structure consists of a superposition of two spectra involving unresolved quadruplets but of similar line shapes. Henceforth we are led to ascribe it to the superposition of two defects, ST1 and ST2, of trigonal symmetry centered on $I=\frac{3}{2}$ nuclei.

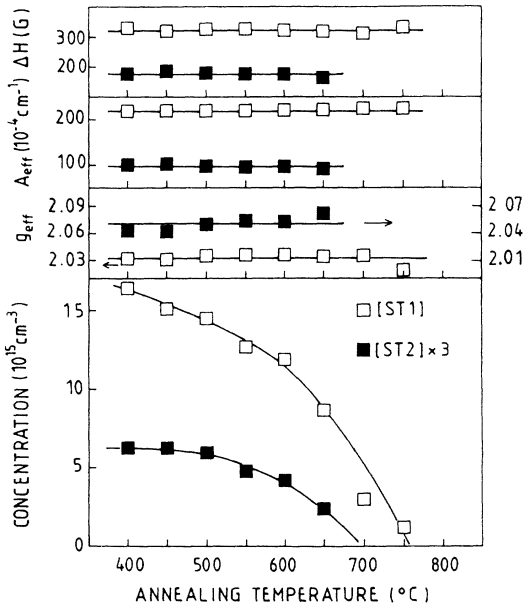

FIG. 9. Variations of the ST1 and ST2 contents as a function of annealing temperature and corresponding variations of the spin Hamiltonian parameters.

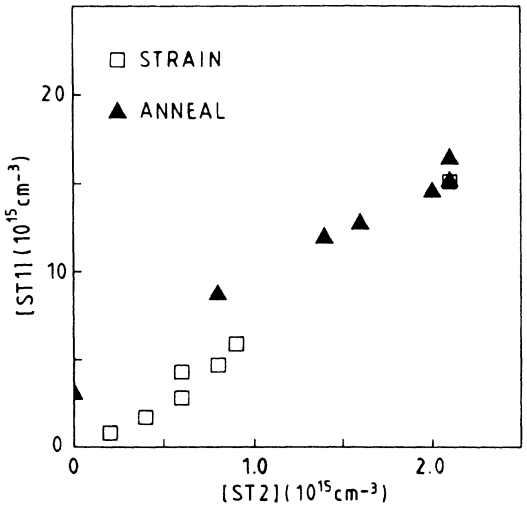

FIG. 10. Correlations between ST1 and ST2 contents during their generation by plastic deformation and their decay during the thermal anneal.

Observation of the ST structure has been confirmed by another group,[6] although there is not yet full agreement on the interpretation of the experimental data. There is, however, consent that ST is not likely a single defect. The alternative solution of a tetragonal center implies an additional singlet. In this case the degeneracy of all branches would occur for $\mathbf{H}_0 \| [111]$. We have rejected this solution for the reasons exposed above.

Actually both symmetries are easily derived from the basic tetrahedral patterns, i.e., A-B_4 or B-A_4 tetrahedra, as found in the sphalerite structure of a binary compound $A^N B^{8-N}$ like GaAs. Substitution of either four nearest neighbors by a different atom (or a vacancy) yields a local trigonal symmetry, whereas the substitution of two of them by two others of a same species leads to long-range tetragonal ordering as found in chalcopyrite compounds such as $A^{II}B^{IV}C_2^{IV}$ ternaries and related structures.[11]

Assignment of an overall defect configuration for ST1 and ST2 requires us to identify the chemical nature of the $I=\frac{3}{2}$ nuclei and guess probable associated partners, responsible for the breaking of the tetrahedral symmetry of the GaAs lattice into a trigonal one.

Pointing out the amazing correlation between the ST1 and ST2 contents both during generation and thermal decay as shown in Fig. 10, we first look for a pair of isotopes. Indeed, the isotropic fraction of the central hyperfine constant may be written as

$$A = k\frac{\mu}{I}|\psi_{(0)}|^2 , \quad (3)$$

where k is a constant depending on the ionicity of the crystal; μ and I are, respectively, the nuclear magnetic moment and spin of the defect nucleus; $\psi_{(0)}$ denotes the electronic density at the core of the defect. For a pair of isotopes, we then expect the ratio of the A values of ST1 and ST2 to be proportional to the ratio of the μ values, whereas their relative intensities would mirror the isotopic abundances.

However, a systematic screening of all elements and their isotopes with $I=\frac{3}{2}$ does not yield a solution satisfying the double constraint set by our experimental data. Therefore, we are led to search for an independent ascription for each defect.

The list of extrinsic species with $I=\frac{3}{2}$ having a natural isotopic abundance of at least 50% contains such elements as Li, Na, Cu, Ir, Be, Cl, Br, Au, B, K, and Tb. B and Cu are of particular interest as they could result from unintentional contaminations. If B could be linked to the B_2O_3 encapsulation or BN crucible for Czochralski-pulled crystal, its presence in Bridgman-grown materials without the former raises a problem. Cu—which has two isotopes,^{63}Cu and ^{65}Cu, with natural abundances of, respectively, 69% and 31%—would require each spectrum to be splittable accordingly. As with most transition metals analyzed by secondary-ion mass spectrometry, the Cu content could be considerably undervalued. On the other hand, EPR, is only sensitive to defects in proper ionization state where they are paramagnetic; in other words, this technique determines only a lower limit for the total content of an extrinsic species. Observation of ST contents much higher than ours as reported by other authors[6] discourages an assignment to extrinsic defects. Besides the association of ST1 and ST2 with physical perturbations may also hint at an intrinsic origin for these spectra.

Henceforth we have to consider the elements of the matrix; Ga has two isotopes—^{69}Ga and ^{71}Ga—with respective 60% and 40% abundances; ^{75}As is 100% abundant. All the former isotopes have $I=\frac{3}{2}$ nuclear spins. We shall discard Ga on the grounds that it would lead to a superposition of two overlapping spectra for either ST1 or ST2, as in the case of Cu. In fact, this argument is even stronger for Ga than for Cu as the ratio of the magnetic moments $\mu(^{71}\mathrm{Ga})/\mu(^{69}\mathrm{Ga})\simeq 1.27$ is larger.

Regarding ^{75}As, the only remaining possible choice, we must define its location at either a substitutional or interstitial site. Assuming that the substitutional anion antisite As_{Ga} has been correctly ascribed,[12–14] there are two locations for an As_i interstitial in a sphalerite structure depending on the nature of the four nearest neighbors. We shall denote them As_i-As_4, and As_i-Ga_4. While these two sites could account for the existence of two similar defects, they fall short without further information for a respective attribution to either ST spectrum.

In order to cope with the requirement of a symmetry along a ⟨111⟩ direction, we suggest the following totally intrinsic binary complexes: As_i-Ga_3V_{Ga}, As_i-GaV_{Ga_3}, As_i-As_3V_{As}, and As_i-AsV_{As_3}. Here we implicitly admit that the presence of a vacancy permits an anisotropy in the electronic configuration in contrast to the As_{Ga}^{+} vacancy-related complexes.[5] In absence of corresponding theoretical calculations, we may argue that the ST configurations no longer correspond to predominant S states on the grounds of their strong coupling with the host lattice as revealed by their microwave-saturation behavior. Of course, such strictly symmetry-based complexes could also be proposed with an extrinsic partner instead of a vacancy, but it would raise the problem of its concentration, as mentioned before.

In fact, the symmetry requirement can also be met by some ternary complexes which are derivable from the former As_i vacancy-related complexes, provided that they share a common ⟨111⟩ direction:

$$V_{As}As_3\text{-}As_i\text{-}Ga_3V_{Ga},\ V_{As}As_3\text{-}As_i\text{-}GaV_{Ga_3},$$

$$V_{As_3}As\text{-}As_iGa_3V_{Ga},\ \text{and}\ V_{As_3}As\text{-}As_i\text{-}GaV_{Ga_3}.$$

Some of the former binary or ternary complexes can probably be discarded on grounds of their overly large stoichiometry deviation or their incompatibility with the usual As excess in melt-grown GaAs. This approach leaves us essentially with the binary complex As_i-Ga_3V_{Ga} and the ternary complex $V_{As}As_3$-As_i-Ga_3V_{Ga}, both corresponding to a single-As-atom excess. However, this success in reducing the number of possibilities may only be apparent as the ternary complex has two possible configurations depending on whether the As interstitial is centered on either the defect As or on the Ga tetrahedron. The slightly different slopes between the ST1 and ST2 correlations during generation and thermal decay depicted in Fig. 10 could perhaps hint at a preferential move of the As interstitial towards the ST1 configuration as the temperature is raised.

Besides the ternary complex $V_{As}As_3$-As_i-Ga_3V_{Ga}, in short $V_{As}As_iV_{Ga}$ is also attractive as it could represent a precursor state of the simultaneously revealed $As_{Ga}V_{As}V_{Ga}$ complex, which we believe is the nearest configuration of the paramagnetic anion antisites generated during plastic deformation.[4] Figure 11 shows the correlations between the As_{Ga}^{+} and ST1 contents during increasing strain and during thermal decay. We have recently demonstrated ST1 to be an acceptor that is neutral in its paramagnetic state, i.e., $ST1^0$.[15]

Roughly estimating that the electrical compensation is determined by the predominant intrinsic species As_{Ga} and further taking into account the data of Fig. 11, we get

$$[As_{Ga}^{+}]\simeq[ST1^{-}]\simeq 2[ST1^{0}] . \quad (4)$$

Therefore we infer that the Fermi level is slightly above the $ST1^{0/-}$ acceptor level in the strained materials, whereas the deep As_{Ga} donors are fully ionized. This result is in agreement with the preliminary observations that heavily deformed or irradiated materials do not show the peculiar increase of the As_{Ga}^{+} signal at short illumination times appropriate for materials in which the deep donors are not fully ionized.[15]

As a compensated acceptor and a precursor of the

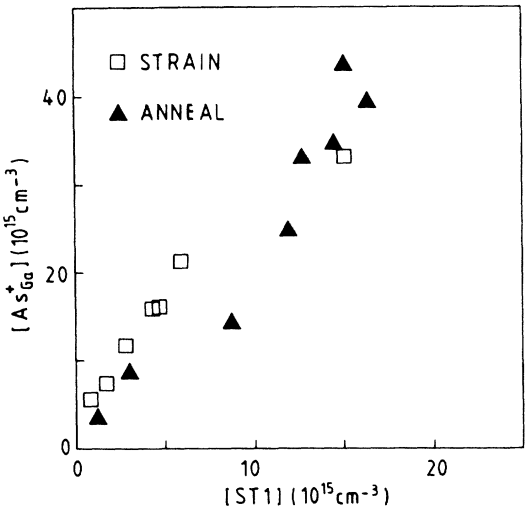

FIG. 11. Correlations between $ST1^0$ and As_{Ga}^{+} contents during plastic deformation and thermal anneal.

$As_{Ga}V_{As}V_{Ga}$ complex, it is reasonable that the parallel relation between the concentrations of $ST1^0$ and As_{Ga}^{+} in Fig. 11 and the electrical compensation may be interpreted by means of a conversion reaction between $V_{As}As_iV_{Ga}$ and $As_{Ga}V_{As}V_{Ga}$, via the $(V_{Ga})_2$ divacancy as follows:

$$2V_{As}As_iV_{Ga} \rightleftarrows (V_{Ga})_2 \rightleftarrows As_{Ga}V_{As}V_{Ga} \ . \quad (5)$$

Other experiments have also led investigators to suspect the existence of As_i defects. It has been speculated recently that the direct infrared-absorption spectra of electron-irradiated GaAs should involve a complex coupling an As_i with a nearby unidentified defect.[16] However, strongest evidence for As_i-related complex stems from the analysis of the localized vibrational modes (LVM)'s due to substitutional C_{As} and B_{Ga} defects in particle-irradiated GaAs.[17] Whereas the C_{As}-As_i pair is likely to be of trigonal symmetry, the B_{Ga}-As_i pair has lower than axial symmetry. Either ST1 or ST2 has the correct symmetry to be identified with a C_{As}-As_i pair, but, as stated before, such an identification requires equal concentrations of both the intrinsic and the extrinsic species. Fairly large amount of As_i, though limited by the initial stoichiometry deviation, may be created during combined climb-glide motion of dislocations in the sphalerite-structured GaAs,[18] but the ubiquitous C content is usually reported as less than 10^{16} cm^{-3}. To our knowledge, LVM measurements on plastically deformed materials have not yet been reported, leaving open the important question of the preexisting content of As_i in the as-grown material and its variation with plastic deformation.

The recent reinterpretation of the optically detected electron-nuclear double resonance (ODENDOR) experiments[19] on the As_{Ga}^{+} center in as-grown p-type GaAs elicits convincing evidence for an As_{Ga}-As_i pair of trigonal symmetry, with the As_i being situated at the second-nearest interstitial site centered on an As tetrahedron. Hence its microscopic structure may be described as an $(As_{Ga}$-$As_4)$-$(As_i$-$As_4)$ complex aligned along a [111] axis.

In fact, the latter complex fully meets the constraints of a trigonal symmetry and a totally intrinsic nature which we are requiring for the ST1 or ST2 ascription. We are thus confronted with the obvious challenge of whether ODENDOR experiments detect the As_{Ga} and whether EPR measurements detect the As_i, with both probes belonging to the same complex. This issue is particularly important in view of the close analogy between the properties of paramagnetic grown-in and deformation-induced anion antisites both from qualitative and quantitative standpoints.[20] According to Meyer,[21] the complex is detected as an As_{Ga}^{+}-As_i pair with a resulting zero electron spin by ODENDOR, leading to an As_{Ga}^{+}-As_i^{+} configuration for the singly ionized pair. On the other hand, we know ST1 to be an acceptor that is paramagnetic in its neutral state; we therefore infer that As_{Ga}-As_i^{0} is the pair seen in EPR, with the electrical state of the As_{Ga} donor, in principle, undetermined. However, as an increasing amount of acceptors is revealed during deformation, we may safely assume that a large fraction (if not all) of the As_{Ga} are ionized. In other words, we expect a majority of As_{Ga}^{+}-As_i^{0} complexes, although some As_{Ga}^{0}-As_i^{0} pairs could also be present at lower strain values.

The observation of different electrical states of the As_{Ga}-As_i pair, i.e., As_{Ga}^{+}-As_i^{+} by ODENDOR and As_{Ga}^{+}-As_i^{0} by regular EPR, does not necessarily imply some contradiction as yet. In the as-grown material studied by ODENDOR, the fraction of ionized acceptors may predominate, while in the deformed samples investigated by regular EPR the neutral acceptors may be the major species. Thus the preferential observation of either pair would only mirror the relative amounts of ionized and neutral As_i acceptors in different samples. As an alternative explanation, the strong interaction between two paramagnetic centers in an As_{Ga}^{+}-As_i^{0} pair may also potentially account for the lack of a corresponding signal in ENDOR experiments.

It has been recently suggested that an optically induced displacement of As_i along a [111] axis is at the origin of the change of configuration of the As_{Ga}-As_i pair during its transfer from the normal to the metastable state of the grown-in As_{Ga}-related defects, eventually leading to its identification with the deep donor EL2 revealed by deep-level transient spectroscopy and displaying a similar peculiarity.[22] According to this model, the stable configuration would correspond to the As_i in a second-neighbor position, i.e., $(As_{Ga}$-$As_4)$-$(As_i$-$As_4)$, whereas in the metastable one the As_i would be in first-neighbor position $(As_{Ga}$-$As_4)$-$(As_i$-$Ga_3As_{Ga})$.

Although this model has stimulated a lively debate, it has not reached general consensus in acceptability. In this context, and provided that our own ST attribution is correct, the existence of an alternative paramagnetic probe, directly linked to the critical As_i species, should pave the way for its further experimental assessment.

[1]E. Christoffel, A. Goltzené, C. Schwab, Wang Guangyu, and Wu Ju, in *Proceedings of the International Conference on Semi-Insulating III-V Materials, Malmö, 1988,* edited by G. Grossmann and L. Ledebo (Hilger, Bristol, 1988), p. 401.

[2]A. Goltzené, B. Meyer, C. Schwab, R. B. Beall, R. C. Newman, J. E. Whitehouse, and J. Woodhead, J. Appl. Phys. **57**, 5196 (1985).

[3]A. Goltzené, B. Meyer, C. Schwab, S. G. Greenbaum,, J. R. Wagner, and T. A. Kennedy, J. Appl. Phys. **56**, 3394 (1984).

[4]S. Benakki, A. Goltzené, C. Schwab, Wang Guangyu, and Zou Yuanxi, Phys. Status Solidi B **138**, 143 (1986).

[5]Wang Guangyu, Zou Yuanxi, S. Benakki, A. Goltzené, and C. Schwab, J. Appl. Phys. **63**, 2595 (1988).

[6]M. Wattenbach, J. Krüger, C. Kieslowski-Kemmerich, and H. Alexander, in *Proceedings of the 15th International Conference on Defects in Semi-conductors, Budapest, 1988,* edited by G. Ferenczi (Trans Tech, Aedermannsdorf, Switz., 1989), Vols. 38–41, p. 73.

[7]E. Christoffel, A. Goltzené, C. Schwab, Wang Guangyu, and Wu Ju (unpublished).

[8]A. Goltzené, B. Meyer, and C. Schwab, J. Appl. Phys. **57**, 1332 (1985).

[9]A. Goltzené, G. Poiblaud, and C. Schwab, J. Appl. Phys. **50**, 5425 (1979).

[10]A. Goltzené, B. Meyer, and C. Schwab, J. Appl. Phys. **53**, 4541 (1982).

[11]E. Parthé, *Cristallo-chimie des structures tétrahédriques* (Gordon and Breach, New York, 1972).

[12]R. J. Wagner, J. J. Krebs, G. H. Stauss, and A. M. White, Solid State Commun. **36**, 15 (1980).

[13]N. K. Goswami, R. C. Newman, and J. E. Whitehouse, Solid State Commun. **40**, 473 (1981).

[14]R. Wörner, U. Kaufmann, and J. Schneider, Appl. Phys. Lett. **40**, 1941 (1982).

[15]E. Christoffel, A. Goltzené, and C. Schwab, J. Appl. Phys. **66**, 5648 (1989).

[16]M. O. Kanasreh and D. W. Fischer, Appl. Phys. Lett. **53**, 2429 (1988).

[17]J. D. Collins, G. A. Gledhill, R. Murray, P. S. Nandrha, and R. C. Newman, Phys. Status Solidi B **151**, 469 (1989).

[18]T. Figielski, Appl. Phys. A **36**, 217 (1985).

[19]B. K. Meyer, D. M. Hoffmann, J. R. Niklas, and J. M. Spaeth, Phys. Rev. B **36**, 1332 (1987).

[20]A. Goltzené and C. Schwab (unpublished).

[21]B. K. Meyer, Rev. Phys. Appl. **23**, 809 (1988).

[22]H. J. von Bardeleben, D. Stievenard, D. Deresmes, A. Huber, and J. C. Bourgoin, Phys. Rev. B **34**, 7192 (1986).